Finite element model based spatial linearity correction for scintillation detectors that use position sensitive avalanche photodiodes

Peter D. Olcott, *Member, IEEE,* Jin Zhang, *Member, IEEE,* Craig S. Levin, *Member, IEEE,* Frezghie Habte, *Member, IEEE,* and Angela M. K. Foudray, *Member, IEEE*

***Abstract*— We have developed a method using polynomial correction derived from a finite element model (FEM) to correct spatial linearity of scintillation detectors that use position sensitive avalanche photodiodes (PSAPD). A PSAPD is a planar avalanche photodiode with a resistive coating that allows continuous, but non-linear, positioning of scintillation light pulses over the entire active area. The spatial response of a scintillation crystal array coupled to a PSAPD shows a characteristic pincushion distortion when using a linear center of mass positioning calculation. A finite element simulation was used to derive the spatial response function for the PSAPD detector, and then used to calculate a polynomial linearity correction. We performed spatial linearity correction of several flood histograms from a ^{22}Na point source on discrete, scored and continuous crystal arrays of lutetium orthosilicate (LSO). For discrete arrays, spatial linearity correction improves crystal segmentation by correcting the pincushion distorted peaks in the 2-D crystal positioning histogram. For continuous sheets, spatial linearity correction allows for linear positioning over the central part of the crystal array without the use of time consuming spatial calibration measurements.**

***Index Terms*— Linearity, Finite Element Model, Position Sensitive Avalanche Photodiode, PSAPD**

I. Introduction

A Semiconductor photodetector converts the scintillation light into a charge density distribution of electron-hole pairs. After amplification from an avalanche process, the charge density will create a 2-D potential distribution on the resistive sheet on the back of the position sensitive avalanche photodiode (see Fig. 1). Using a linear center of mass positioning algorithm, the resistive sheet has a non-linear mapping between event location and detected position. With the assumption that the entire process from scintillation light through event positioning may be described as a mapping (one-to-one and onto), the operator that maps the event position to detected position can be inverted to remove the positioning non-linearity. A Positive Sensitive Avalanche photodiode(PSAPD) uses a resistive sheet to split the charge into four corner contacts [1], [2]. The spatial response of the PSAPD to scintillation events has a non-linear pincushion distortion. By solving the ideal spatial response function of a resistive sheet charge division readout, the spatial response can be corrected and made more linear. A more linear spatial response helps simplify crystal segmentation. It can also be used to provide linear positioning for a sheet crystal.

Manuscript received November 11, 2005; This work was funded in part by NIH R21 EB003283 and NIH R21 CA098691.

P. Olcott, Frezghie Habte, C. Levin, A. Foudray are with the Department of Radiology and the Molecular Imaging Program at Stanford University. A. Foudray is also with the Department of Physics at the University of California at San Diego. Jin Zhang is now working for PerkinElmer.

TABLE I
Definitions

$L^{positioning}$	Positioning operator
$L^{detector}$	Charge potential operator
$L^{crystal}$	Light distribution operator
$\phi(\vec{\mathbf{x}})$	Light photon density distribution for a single event
$Q(x,y)$	2-D potential
$\vec{E}$	Electric field
$\vec{J}$	Current density
$\vec{\mathbf{x}}$	Event location
∇	Gradient
Δ	Laplacian
$\delta_0(\vec{\mathbf{x}})$	Offset delta function
Ω_{square}	Square sheet domain
$\partial\Omega$	Boundary of square sheet domain
$\vec{\mathbf{c}}$	Corner contacts of boundary sheet domain
I	Current
$P_0,\ P_1$	4 channel projection matrices
$\vec{\mathbf{y}}$	PSAPD event location
$\langle L^{poly}_{order} \mid \cdot \rangle$	2-D Polynomial expansion operator
A	Polynomial linearity correction coefficient
$\hat{\mathbf{y}}$	PSAPD event location expanded onto polynomial basis
$\vec{\mathbf{y}}_{\mathbf{meas}}$	Measured event position
$\hat{\mathbf{y}}_{\mathbf{meas}}$	Measured event position expanded onto polynomial basis

II. Spatial response of a PSAPD

A gamma ray interaction in the scintillation crystal volume will create a light distribution centered at $\vec{\mathbf{x}}$ that is converted into a charge density $\phi(\vec{\mathbf{x}})$ and amplified by the avalanche process in the PSAPD detector.

$$\phi(\vec{\mathbf{x}}) = \langle L^{crystal} \mid \vec{\gamma}(x,y,z) \rangle \tag{1}$$

The charge distribution centered at $\vec{\mathbf{x}}$ will form a 2-D potential, $Q(x,y)$ on the resistive sheet of the PSAPD.

$$Q(x,y) = \langle L^{detector} \mid \phi(\vec{\mathbf{x}}) \rangle \tag{2}$$

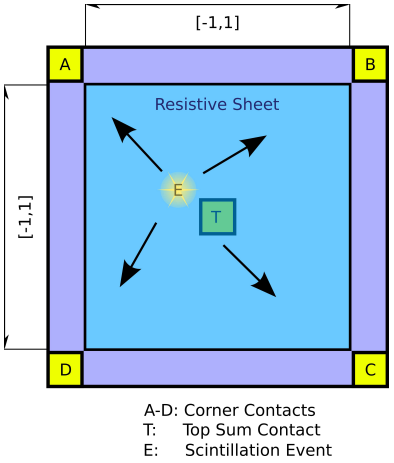

Fig. 1. The PSAPD is a planar avalance photodiode with a resistive sheet patterned on the backside of the device. 4 corner contacts are fabricated on the top of the resistive sheet. Charge sensitive preamplifiers amplify the charge collected from the corners. The energy, position, and time of a scintillation event can be determined by digitizing the the 4 channels.

By reading out the 4 corners of the resistive sheet, the 2-D potential will map to the detected event position $\vec{\mathbf{y}}_{\mathbf{meas}}$ with the pincushion distortion.

$$\vec{\mathbf{y}}_{\mathbf{meas}} = \langle L^{positioning} \mid Q(x,y) \rangle \tag{3}$$

If we assume $\left(L^{crystal} \circ L^{detector} \circ L^{positiong}\right)$ is one-to-one and onto, we can solve for the potential on the resistive sheet and use this to correct for the non-linear spatial response due to the resistive sheet. Poisson's Heat equation can be used to describe the relation between the injected charge on a resistive sheet and the potential on the surface as a function of space and time. If the parasitic capacitance of the photodiode is assumed to be much smaller than that of the resistive sheet, Poisson's heat equation reduces to the steady state Laplace's equation.

$$Q(x,y) = \Re \ , \quad \vec{\mathbf{x}} = \langle x,y \rangle \in \Omega_{square} \tag{4}$$

$$\vec{E} = \nabla Q \ , \quad \nabla \equiv \langle \frac{\partial}{\partial x}, \frac{\partial}{\partial y} \rangle \ , \quad \vec{E} = \sigma \cdot \vec{J}, \tag{5}$$

$$\nabla \cdot \vec{E} = 0 \ , \ \ \nabla \cdot (\nabla Q) = 0 \ , \ \ \Delta Q = 0 \ , \ \ \Delta \equiv \frac{\partial^2}{\partial^2 x} + \frac{\partial^2}{\partial^2 y} \tag{6}$$

Since Laplace's equation is linear under a center of mass calculation, we can replace the non-uniform, circularly symmetric charge distribution of a scintillation event as a single point injection at $\vec{\mathbf{x}}$ of steady state current.

$$\Delta Q = \delta_0(\vec{\mathbf{x}}) \tag{7}$$

The ratio of charge collected by each of the 4 corner contacts can be determined by the solution of Laplace's equation on a square sheet with insulating boundaries and corner contacts.

$$\nabla Q \cdot \vec{\mathbf{n}} = 0 \ , \quad \vec{\mathbf{n}} = \partial\Omega \tag{8}$$

The corner contacts are modeled as fixed ground potentials.

$$Q(\vec{\mathbf{c}}) = 0 \ , \quad \vec{\mathbf{c}} = \{\langle -1,-1 \rangle \ , \ \langle -1,1 \rangle \ , \ \langle 1,-1 \rangle \ , \ \langle 1,1 \rangle\} \tag{9}$$

The charge recorded by a spatial channel is proportional the magnitude of the of the current density field evaluated at the corner.

$$I(\vec{\mathbf{c}}) \propto \|J(\vec{\mathbf{c}})\| \tag{10}$$

$$I(\vec{\mathbf{c}}) \propto \frac{1}{\sigma} \|\nabla Q(\vec{\mathbf{c}})\| \ , \quad I \equiv \frac{1}{\sigma} \sqrt{\left(\frac{\partial}{\partial x}\right)^2 + \left(\frac{\partial}{\partial y}\right)^2} \tag{11}$$

III. Finite Element Simulation

Finite element simulation (FEM) can be used to solve Laplace's equation using finite differences on the square $(-1,1)$. For each position $\vec{\mathbf{x}} \in < x,y >$ on the square, an impulse of current is injected and the potential is solved over a 201x201 element grid (see Fig. 2(a)). The magnitude of the current densities evaluated at the corners for each discretized event position are recorded as the corner spatial signals.

$$\begin{aligned} \dot{\mathbf{a}} &= I(\langle -1,1 \rangle) \\ \dot{\mathbf{b}} &= I(\langle 1,1 \rangle) \\ \dot{\mathbf{c}} &= I(\langle 1,-1 \rangle) \\ \dot{\mathbf{d}} &= I(\langle -1,-1 \rangle) \end{aligned} \tag{12}$$

The corner spatial signals for channels A through D are then projected onto a 2-D coordinate space, $\vec{\mathbf{y}}$, using projections P0 and P1 defined in Eq. 14 and 15. For each event position on a uniform grid $\vec{\mathbf{x}}$, we now have a detected event position $\vec{\mathbf{y}}$.

$$\vec{\mathbf{y}} = \frac{P_0[\ \dot{\mathbf{a}}\ \dot{\mathbf{b}}\ \dot{\mathbf{c}}\ \dot{\mathbf{d}}\ ]}{P_1[\ \dot{\mathbf{a}}\ \dot{\mathbf{b}}\ \dot{\mathbf{c}}\ \dot{\mathbf{d}}\ ]} \tag{13}$$

$$P_0^{lin} = \begin{bmatrix} 1 & 1 \\ -1 & 1 \\ 1 & -1 \\ -1 & -1 \end{bmatrix}, \quad P_1^{lin} = \begin{bmatrix} 1 & 1 \\ 1 & 1 \\ 1 & 1 \\ 1 & 1 \end{bmatrix} \tag{14}$$

$$P_0^{ratio} = \begin{bmatrix} 1 & 0 \\ 0 & 1 \\ -1 & 0 \\ 0 & -1 \end{bmatrix}, \quad P_1^{ratio} = \begin{bmatrix} 1 & 0 \\ 0 & 1 \\ 1 & 0 \\ 0 & 1 \end{bmatrix} \tag{15}$$

We have identified two different projectors for the positioning calculation (see Eq. 14 and Eq. 15). The first projector (Eq. 14) corresponds to the standard weighted mean of the four corner signals to obtain position $((a-b)+(c-d)/sum)$ and $(a-c)+(b-d)/sum)$ and leads to the spatial response in Fig. 2(b). The second projector (Eq. 15) corresponds to only using two diagonally opposed corner signals at a time for positioning $((a-c)/(a+c)$ and $(b-d)/(b+d))$ and leads to the spatial response in Fig. 2(c). Both of these methods suffer from spatial non-linearity.

IV. Linearity Correction

The spatial response between the event position and the detected position can be inverted to provide a linearity correction. The detected position can be expanded using a 2-D polynomial basis. The coefficients, A, that map from the expansion onto a the uniform grid can be solved by using the pseudo-inverse.

$$\hat{\mathbf{y}} = \langle L_{order}^{poly} \mid \vec{\mathbf{y}} \rangle \equiv \left[\vec{\mathbf{y}}\ \vec{\mathbf{y}}^{\mathbf{2}}\ \vec{\mathbf{y}}^{\mathbf{3}}\ \cdots\ \vec{\mathbf{y}}^{\mathbf{order}}\right] \tag{16}$$

$$A\hat{\mathbf{y}} = \vec{\mathbf{x}} \tag{17}$$

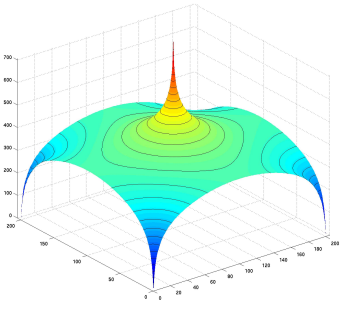

(a) 2-D potential solved for a point injection of current at the center

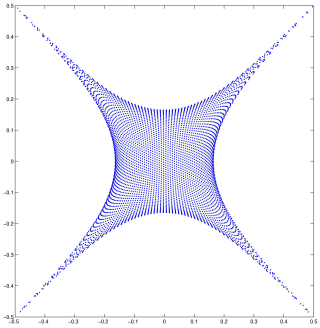

(b) Linear center of mass projection spatial response using P_0^{lin} and P_1^{lin}, Eq. 14

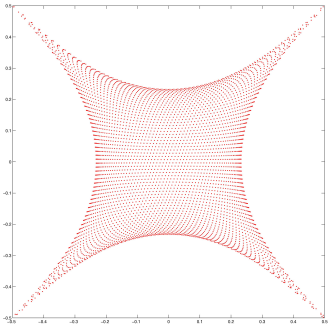

(c) Ratio projection spatial response using P_0^{ratio} and P_1^{ratio}, Eq. 15

Fig. 2. The FEM simulation is run for every possible event position and the 2-D potential (Fig. 2(a)) is calculated. The spatial response function is determined from projection from the 4 channels onto a $< x, y >$ plane (Figs. 2(b) and 2(c)). The pincushion distortion is present for both projections, but has more non-linearity for linear (blue Fig. 2(b)) than corner ratio (red Fig. 2(c)) calculation.

$$A = \vec{\mathbf{x}}\hat{\mathbf{y}}^{\mathbf{T}}\left(\hat{\mathbf{y}}\hat{\mathbf{y}}^{\mathbf{T}}\right)^{-\mathbf{1}} \tag{18}$$

Measured events $\vec{\mathbf{y}}_{\mathbf{meas}}$ expanded onto the same 2-D polynomial basis $\hat{\mathbf{y}}_{\mathbf{meas}}$ can be corrected by multiplication by the correction coefficients A.

$$A\hat{\mathbf{y}}_{\mathbf{meas}} \cong \vec{\mathbf{x}} \tag{19}$$

V. Experimental Materials and Methods

We tested the polynomial correction technique and several ^{22}Na flood histograms of cerium-doped lutetium oxyorthosilicate(LSO) [3] scintillation crystals coupled to a 8 mm x 8 mm PSAPD device. We are using these arrays for high performance positron emission tomography applications [4], [5]. The device was biased to -1740V at room temperature. The device was readout using 4 Cremat 110 preamplifiers connected to a 500 ns Gaussian shaper and 4 channel National instruments DAQ. The continuous sheet consisted of a 8 mm x 8 mm x 1 mm LSO crystal that was coupled to the device using optical grease and covered with several layers of Teflon reflector. We also used an 8 x 3 array of 1 mm x 1 mm x 3 mm LSO crystals with the large face (1 mm x 3 mm) of each crystal coupled to the device. Lastly, we used a 2-D scored sheet crystal of 8 mm x 8 mm x 2 mm. A 2-D scored sheet crystal [6] has a pattern of 8 cuts on a 1 mm pitch by 2 cuts on a 3 mm pitch on the top surface that are 1 mm deep. On the bottom surface, there are a pattern of 7 cuts on a 1 mm pitch by 3 cuts that are offset by 500 μm and 1.5 mm, respectively, from the cuts of the upper surface. The spatial encoded light sharing determines of whether the top 1 mm or the bottom 1 mm can be distinguished by unique peaks created in the flood histogram. We used a 5th order polynomial to fit the spatial response function.

VI. Results

The polynomial correction improved the linearity of the three different crystal geometries(see Fig. 3). The sheet crystal could not be fully corrected because the assumption that the $L^{crystal}$ is an invertible mapping does not hold when there exists scintilaltion light fold back at the edge of the sheet crystal. Fold back exists when two positions map to the same location and will give rise to hot edges in a flood histogram that can be see in Fig. 3(a). The linearity in the 8 x 3 array was substantially improved in Fig. 3(b) which led to improved crystal segmentation. The crystals in 8 x 3 array are rectangular and give rise to non-circular crystal histograms. Automated segmentation of the flood histogram is easier when the crystal peaks are on a more regular grid. The banana shape of the corner crystals is mis-segmented in Fig. 3(b) in the uncorrected flood histogram but correctly segmented in the corrected histogram. It was also easier to identify the crystal histogram peaks in the scored 2-D array in Fig. 3(c) after correction.

VII. Discussion

The simplified assumptions of the FEM model doesn't take into account the significant blurring of the spatial response of the scintillation crystal because of noise in the readout electronics and the PSAPD. Overlaying the flood histograms onto the calculated spatial response function leaves many events outside the domain of the spatial response function. The spatial response is very narrow in the corners in Fig. 2(b). A small amout of noise from the readout or the PSAPD will blur events outside this narrow domain. Events outside of the domain of the spatial response function will be mispositioned when corrected. We chose a low order polynomial so that we didn't have problems if events were slightly outside the domain of the fit. Also, the measured events are also scaled by a constant that makes sure almost all events fall within the domain of the spatial response function. By scaling down the flood histogram, the "gain" or amount of correction is reduced, which is why some non-linearity still remains.

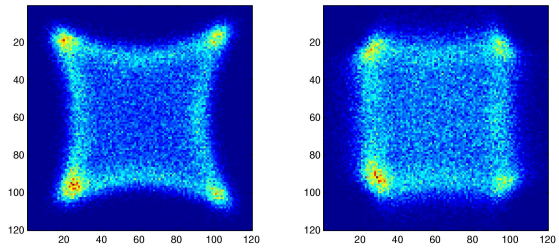

(a) 8 mm x 8 mm x 1 mm continous LSO sheet crystal before and after correction

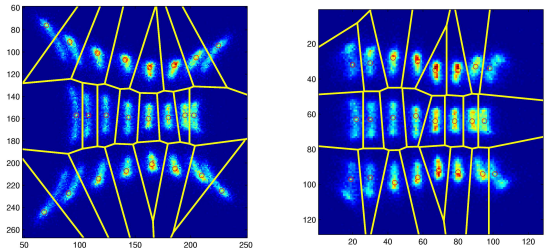

(b) A 8 x 3 array of 1 mm x 1 mm x 3 mm LSO discrete crystals before and after correction

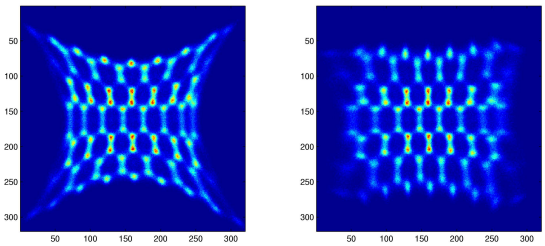

(c) A scored 2-D 8 mm x 8 mm x 2 mm sheet with 500 μm offset 1 mm pitch by 3 mm pitch 500 μm depth cuts before and after correction

Fig. 3. Three different ^{2}2Na flood histograms of LSO scintillation crystals are linearity corrected by a 2-D polynomial derived from FEM simulation. All crystals are placed on the detector with the large area face coupled to the detector. This gives very the best light detection efficiency. The continuous sheet in Fig. 3(a) is only partially corrected since it cannot corrected for the fold back seen at the edges. The sheet crystal does not satisfy the assumption that its operator ($L^{crystal}$) is an invertible mapping (one-to-one and onto) because around the edge there are 2 or more positions that map to the same location. Linearity correction improves segmentation of discrete crystal arrays (Figs. 3(b) and 3(c)) because it allows simpler boundaries to be draw around crystals.

VIII. Conclusion

The pincushion non-linearity of the PSAPD can be corrected by a polynomial correction. The polynomial correction can be determined from a finite element model solution of Laplace's equation on a insulating sheet with corner contacts. The correction can be used for the inner part of a sheet crystal to provide a more linear mapping between detected position and event position. For discrete crystals, the linearity correction improves crystal segmentation by allowing for simpler boundaries to be drawn around crystals.

Acknowledgment

The authors would like to thank RMD, Inc for fabrication of and useful comments for PSAPD devices.

References

[1] K. S. Shah, R. Farrell, R. Grazioso, R. Myers, and L. Cirignano, "Large-area apds and monolithic apd arrays," *IEEE Trans Nucl Sci*, vol. 48, no. 6, pp. 2352 – 2356, Dec 2001.

[2] K. S. Shah, R. Farrell, R. Grazioso, E. S. Harmon, and E. Karplus, "Position-sensitive avalanche photodiodes for gamma-ray imaging," *IEEE Trans Nucl Sci*, vol. 49, no. 4, pp. 1687 – 1692, Aug 2002, part 1.

[3] C. L. Melcher and J. S. S. and, "Cerium-doped lutetium oxyorthosilicate: a fast, efficient new scintillator," *IEEE Trans Nucl Sci*, vol. 39, no. 4, pp. 502 – 505, Aug 1992.

[4] C. S. Levin, "Design of a high-resolution and high-sensitivity scintillation crystal array for pet with nearly complete light collection," *IEEE Trans Nucl Sci*, vol. 49, no. 5, pp. 2236 – 2243, Oct 2002, part 1.

[5] C. S. Levin, A. M. K. Foudray, P. D. Olcott, and F. Habte, "Investigation of position sensitive avalanche photodiodes for a new high resolution pet detector design," *IEEE Nucl Sci Symp Conf Rec*, vol. 4, pp. 2262 – 2266, Oct 2003.

[6] F. Habte, P. Olcott, C. S. Levin, and A. M. Foudray, "Investigation of scintillation light multiplexing for pet detectors based on position sensitive avalanche photodiodes," *IEEE Nucl Sci Symp Conf Rec*, 2005, to be published.